Thin Solid Films 518 (2010) 7339–7342

Contents lists available at ScienceDirect

Thin Solid Films

journal homepage: www.elsevier.com/locate/tsf

# Nonvolatile memory effect of tungsten nanocrystals under oxygen plasma treatments

Shih-Cheng Chen [a,*], Ting-Chang Chang [b], Wei-Ren Chen [c], Yuan-Chun Lo [d], Kai-Ting Wu [d], S.M. Sze [c], Jason Chen [e], I.H. Liao [e], Fon-Shan Yeh(Huang) [a]

[a] *Department of Electrical Engineering & Institute of Electronic Engineering, National Tsing Hua University, Taiwan, ROC*
[b] *Department of Physics and Institute of Electro-Optical Engineering, and Center for Nanoscience and Nanotechnology, National Sun Yat-Sen University, Taiwan, ROC*
[c] *Institute of Electronics, National Chiao Tung University, Taiwan, Hsinchu, Taiwan 300, ROC*
[d] *Institute of Photonics Technologies, National Tsing Hua University, Taiwan, ROC*
[e] *ProMOS Technologies, No. 19 Li Hsin Rd., Science-Based Industrial Park, Hsinchu, Taiwan 300, ROC*

ARTICLE INFO

Available online 1 June 2010

*Keywords:*
Nonvolatile
Nanocrystals
Memory
Oxygen
Plasma

ABSTRACT

In this work, an oxygen plasma treatment was used to improve the memory effect of nonvolatile W nanocrystal memory, including memory window, retention and endurance. To investigate the role of the oxygen plasma treatment in charge storage characteristics, the X-ray photon-emission spectra (XPS) were performed to analyze the variation of chemical composition for W nanocrystal embedded oxide both with and without the oxygen plasma treatment. In addition, the transmission electron microscopy (TEM) analyses were also used to identify the microstructure in the thin film and the size and density of W nanocrystals. The device with the oxygen plasma treatment shows a significant improvement of charge storage effect, because the oxygen plasma treatment enhanced the quality of silicon oxide surrounding the W nanocrystals. Therefore, the data retention and endurance characteristics were also improved by the passivation.

© 2010 Elsevier B.V. All rights reserved.

## 1. Introduction

Conventional nonvolatile memory (NVM, a flash memory) suffers from limitations on continual scaling of device structures. Therefore, in recent years nanocrystal nonvolatile memory devices have been investigated in an attempt to overcome drawbacks of conventional floating gate memory. Due to discrete traps storage nodes acting as their charge centers, nanocrystal nonvolatile memory devices can effectively avoid data loss under reliability test when scaling down devices [1,2].

In various nanocrystal nonvolatile memories, metal nanocrystals are good candidates for improving the retention property and charge storage ability [3–10], due to their high work function. In this study, tungsten (W) nanocrystals were chosen beside its high work function, their thermal stability is suitable for the process thermal budget [11]. In addition, the density of nanocrystals used in nanoscale devices is also an issue because the memory window is dependent on its density. High density is helpful to scale down device structures. When the density of nanocrystals is very high, the quality of the oxide surrounding nanocrystals becomes critical and the electron storage in those nanocrystals will escape by trap to trap tunneling [12,13]. In order to improve the oxide quality, high pressure hydrogen annealing or high temperature annealing was used [14]. In this work a post-$O_2$ plasma treatment was proposed for tungsten nanocrystal nonvolatile memory in order to passivate the defect and improve the surrounding oxide quality. This treatment has the advantages of a simple fabrication process and small thermal budget. Plasma treatment passivation methods have been widely used for passivation of traps in poly-Si TFTs [15] and they are very compatible with semiconductor fabrication technology. Material and electrical analyses were performed to study the nanocrystal memory with and without the hydrogen plasma treatment.

## 2. Experiment details

In this work, the W nanocrystal NVM capacitor structure was fabricated on a single-crystal 6 inch (100) oriented P-type silicon. It was cleaned by the standard Radio Corporation of America (RCA) process, followed by a thermal oxidative process, to form 5-nm-thick dry $SiO_2$ layer as a tunnel oxide in an Atmospheric Pressure Chemical Vapor Deposition (APCVD) furnace. Afterward, a 4-nm-thick tungsten silicide ($WSi_2$) thin film was deposited onto the tunnel oxide by sputtering at room temperature. The $WSi_2$ film was deposited by sputtering only with argon plasma 50 sccm at a DC power of 100 W. Subsequently, 6-nm-thick amorphous silicon (a-Si) was deposited by the same system with argon plasma 30 sccm and a RF power of 100 W. After the deposit of $WSi_2$/a-Si double layer structure, the high temperature thermal oxidation was performed in the rapid thermal annealing (RTA) system in oxygen ambient. RTA oxidation at 800 °C

* Corresponding author. No. 101, Section 2, Kuang-Fu Road, Hsinchu, Taiwan 30013, ROC.
*E-mail address:* scchen0213@gmail.com (S.-C. Chen).

0040-6090/$ – see front matter © 2010 Elsevier B.V. All rights reserved.
doi:10.1016/j.tsf.2010.04.107

for 60 s is required to allow the $WSi_2$ layer to form tungsten NCs, which were embedded between the tunnel oxide and the control oxide. Afterwards, a 30-nm-thick $SiO_2$ layer was deposited by Plasma-enhanced Chemical Vapor Deposition (PECVD) system to form a thicker control oxide layer. For comparison, some of the samples were treated with oxygen plasma for 30 min by PECVD, with 200 W of plasma power and 200 sccm of gas flow rate at a 300 °C environment, respectively. The sample without plasma treatment is the standard sample. Finally, the top and the bottom Al electrodes were patterned by a shadow mask to form Metal–Oxide–Insulator–Oxide–Silicon (MOIOS) structure. The aluminum was deposited by a thermal evaporator system, with a thickness of 500 nm. Electrical characteristics of the capacitance–voltage (*C*–*V*) hysteresis were also measured by HP4284 Precision *LCR* Meter with a high frequency of 100 kHz. TEM analysis and XPS were adopted for microstructure and chemical material analysis of nanocrystals.

## 3. Results and discussion

Fig. 1(a) and (b) shows the cross-sectional and top-view of the TEM image of the sample structure, respectively. In Fig. 1(a), separate nanocrystals cannot be clearly observed because its density is very high. However, in the top-view of Fig. 1(b), the separate nanocrystal is obvious. From the TEM image analysis, the average diameter of nanocrystals is approximately 8 nm and the area density is $2.5 \times 10^{12}$ $cm^{-2}$.

Fig. 2(a) presents the W 4f core-level photoemission spectra of the standard sample, performed using a monochromatic Al *Kα* (1486.6 eV) X-ray. It consists of two main peaks W $4f^{7/2}$ (31.4 eV) and W $4f^{5/2}$ (33.5 eV). The position of 35.2 eV, where a small peak can be observed, is

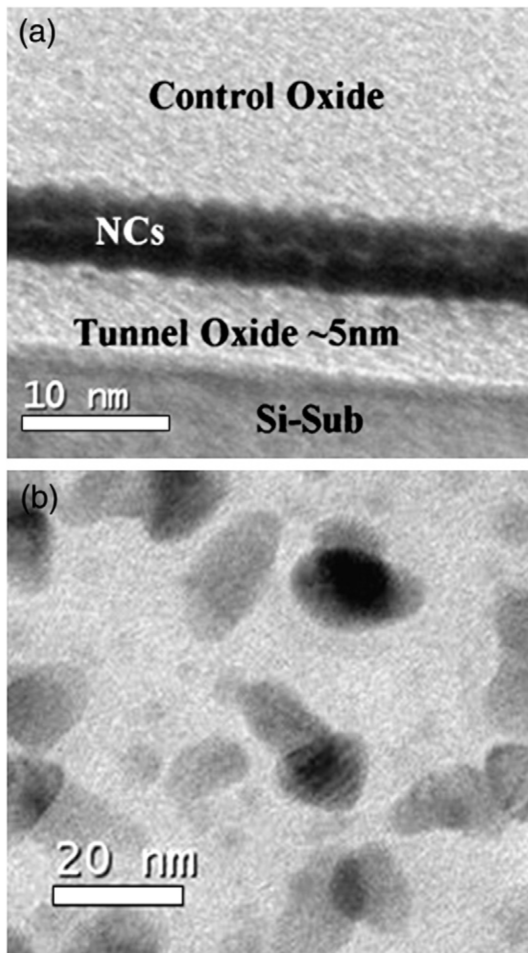


**Fig. 1.** TEM image of tungsten nanocrystal NVMs. (a) Cross-section. (b) Plain-view.

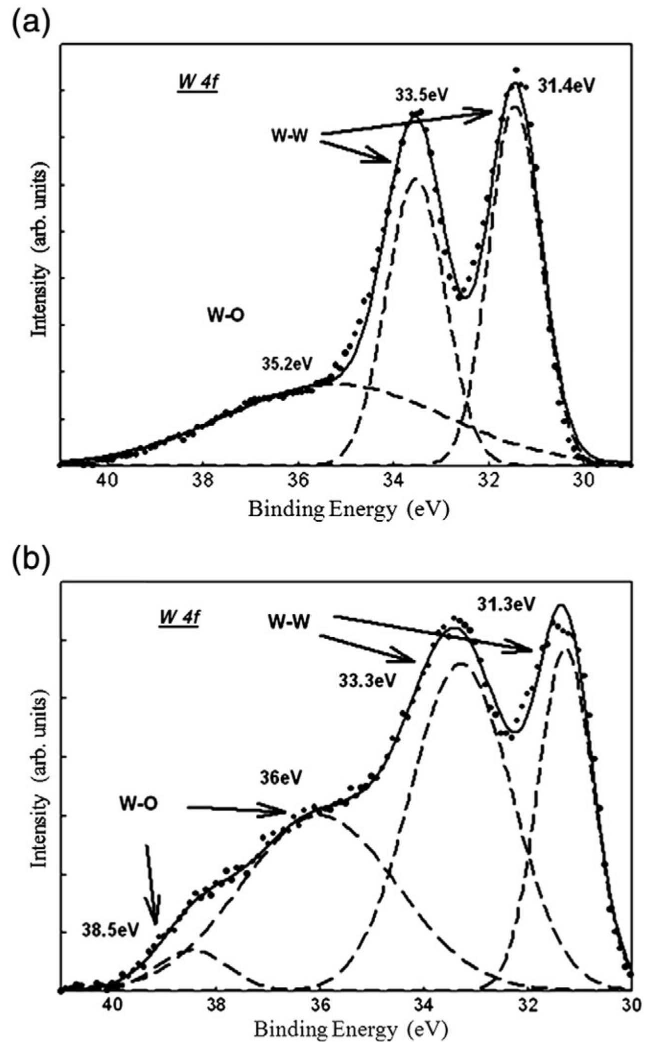


**Fig. 2.** XPS analysis of the W 4f core-level spectrum. (a) Standard sample. (b) Sample with $O_2$ plasma treatment.

the $WO_3$ peak of W 4f bonding [16,17]. Some of the W were oxidized during the rapid thermal annealing in the oxygen ambient. The XPS analysis of W 4f spectra of the sample with the $O_2$ plasma treatment is shown in Fig. 2(b). We can observe a small decrease in the intensity of W $4f^{7/2}$ (31.4 eV) and W $4f^{5/2}$ (33.5 eV), and an increase in $WO_3$ $4f^{7/2}$ (36 eV) and $WO_3$ $4f^{5/2}$ (38.5 eV) [18,19]. Because the solid solubility of O atoms within W material is extremely small [20], O atoms cannot exist in W nanocrystals except in an absolute oxidation of tungsten. Therefore, the position of $WO_3$ should be on the surface of the W nanocrystals. For instance, W nanocrystals may be encapsulated by a very thin $WO_3$ layer [5].

Fig. 3(a) shows the XPS Si 2p spectra of the standard sample, which consists of two main peaks, $Si^{0+}$ (99.7 eV) and $Si^{4+}$ (103.3 eV). As shown in Fig. 3(b), the XPS Si 2p spectra of sample with the $O_2$ plasma treatment only consist of one peak, $SiO_2$ (103.3 eV) [21]. From Fig. 3, we observed that if the sample were treated with the $O_2$ plasma the peak $Si^{0+}$ (99.7 eV) disappeared. This indicates during the plasma treatment, oxygen ions may repair the Si dangling bonds of the surrounding oxide to form Si–O bonds and oxidize Si to $SiO_2$ more completely.

Fig. 4 shows the basic of *C*–*V* hysteresis diagram of the electrical characteristics for both the standard samples and those with the $O_2$ plasma treatment. The solid square is the standard sample (STD) under ±10 V compared to the flat-band gate voltage operation, with a memory window of ~8.8 V. The same comparison for the sample with the $O_2$ plasma treatment has a memory window of 12 V. Because the

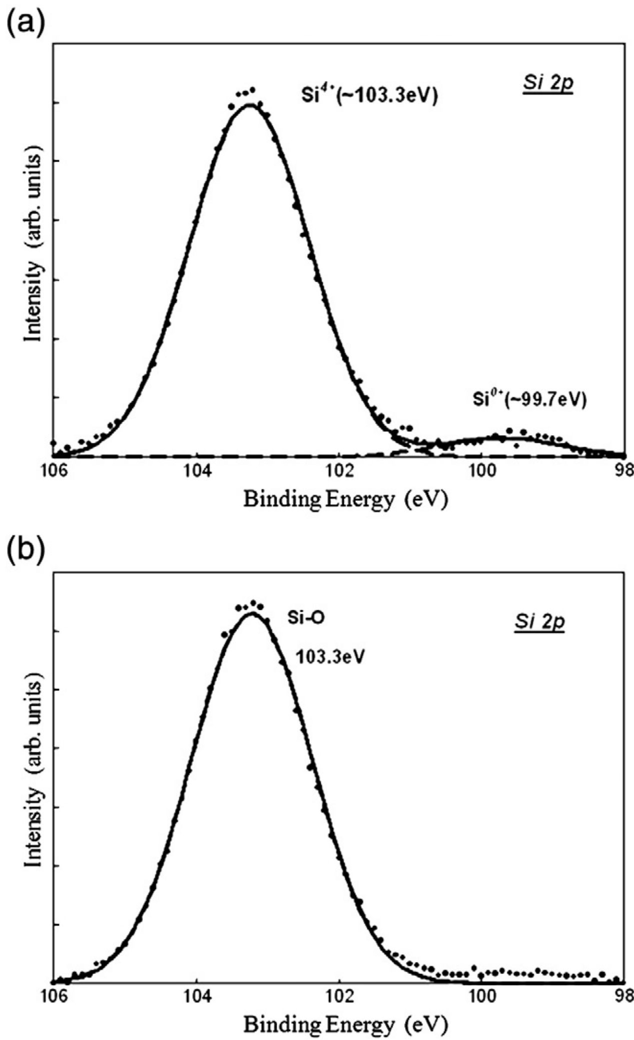


**Fig. 3.** XPS analysis of the Si 2p core-level spectrum. (a) Standard sample. (b) Sample with $O_2$ plasma treatment.

relative concentration ratio of WO/(W+WO) calculated by the integration values of individual peaks only increases by 3% after the plasma treatment, we think this is not the main reason for the improved memory window. In addition, in general, the memory window decreases as the trap density is reduced in SONOS-type memory. Therefore, we suggest that in nanocrystal memories, because charges are mainly stored in nanocrystals, the increase of memory window is due to the improvement of oxide quality surrounding the nanocrystals, suppressing the de-trapping via traps initially, and overall allowing more electrons to be stored in the nanocrystals.

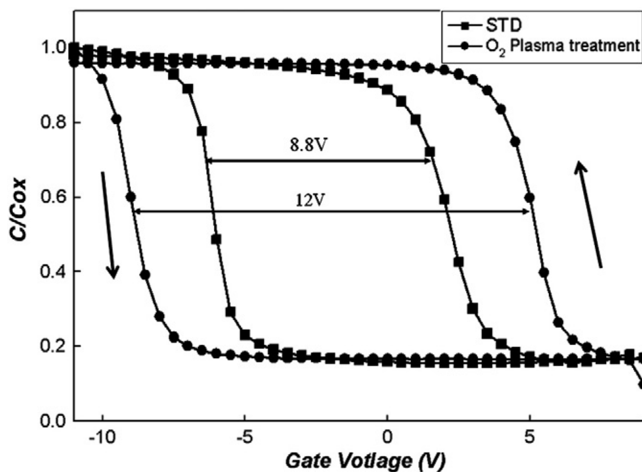


**Fig. 4.** Electrical characteristic of *C–V* hysteresis under ±10 V gate voltage operation.

When the density of nanocrsytals is very high, the isolation layer between two metallic nanocrsytals becomes thin, and because of this, the surrounding oxide quality is important. If the surrounding oxide quality is not good enough to block the lateral electron migration effect, the electron storage in the nanocrsytals will escape, as shown in Fig. 5(a). As can be seen from the XPS analysis, the $O_2$ plasma treatment can oxidize the Si of surrounding oxide to $SiO_2$ and better complete $SiO_2$. The surrounding oxide quality is improved and can effectively reduce the lateral electron migration as shown in Fig. 5(b). Therefore, more large memory windows and more stable endurance performance of the sample with $O_2$ plasma treatment were observed.

Fig. 6(a) and (b) presents the endurance characteristics of standard sample W nanocrsytals and the sample with the $O_2$ plasma treatment under pulse condition of $Vg-Vfb=\pm 7$ V for 10 ms. The flat-band voltage can be defined by using the *C–V* hysteresis under ±7 V gate voltage operation. The memory of standard devices can be distinguished after $10^6$ program/erase cycles at room temperature, however the memory is degraded to about 42.5% as shown in Fig. 6(a). It is because during the endurance test, carriers transport between nanocrystals and the substrate can damage the surrounding oxide. From Fig. 6(b), it was found that the variation of memory window is stable after $10^6$ program/erase cycles for devices with the $O_2$ plasma treatment.

Further analysis of the reliability indicated the charge retention properties of W nanocrystal nonvolatile memory structure at 25 °C for both the standard sample and those with the $O_2$ plasma treatment, demonstrated in Fig. 7(a) and (b), respectively. The memory windows of the two samples were programmed to similar values in the retention measurements. The memory window significantly decays during the first 100 s due to the charge emission from the shallow traps in the SiO*x* matrix to the substrate. However, after 100 s the memory window becomes more stable. In general, if more charges are stored in the traps rather in the nanocrystals, the more serious degradation of memory window can be expected. Therefore, the improved retention characteristic is believed due to the improvement of oxide quality surrounding the nanocrystals. After $10^5$ s, the memory window of the standard sample remained at 35%. The solid circles show the retention property of the sample that has undergone the $O_2$ plasma treatment. The retention properties of the sample with $O_2$ plasma treatment are superior. The memory window is about 60% after $10^5$ s. The enhancement of endurance and retention properties was attributed to the fact that the $O_2$ plasma treatment can repair defects and improve the surrounding silicon oxide quality of W nanocrystals.

## 4. Conclusion

In conclusion, this study investigates the influence of post-oxygen plasma treatment on the electrical characteristics and the chemical

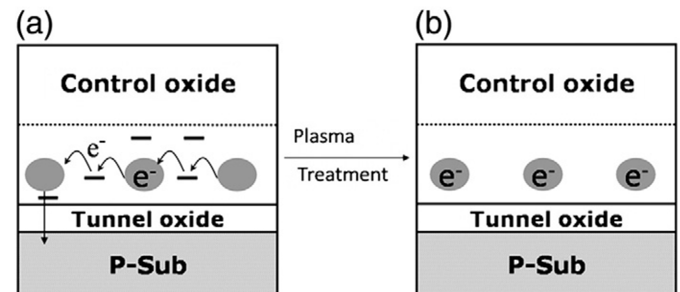


**Fig. 5.** (a) Lateral leakage current phenomenon of non-ideal NC structure. (b) NC structure with plasma treatment.

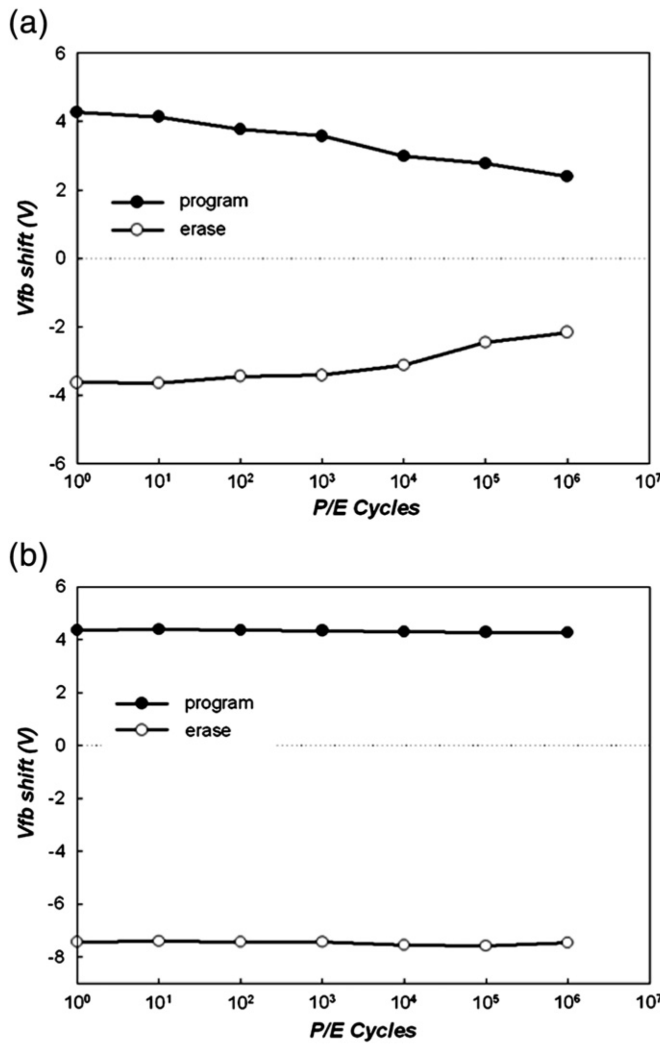


**Fig. 6.** Endurance characteristic of tungsten nanocrystal NVMs (a) without and (b) with the plasma treatment under the pulse conditions of Vg − Vfb = ± 7 V for 10 ms. The flat-band voltage can be defined by using the *C*–*V* hysteresis.

composition of the proposed tungsten nanocrystal nonvolatile memory. After the oxygen plasma treatment, the XPS results indicated that Si dangling bonds (traps) in $SiO_2$ have been repaired by the oxygen passivation. The treatment is able to restrain lateral electron migration by repairing defects, oxidizing oxide more completely and improving the quality of the oxide surrounding the nanocrystals. By using the oxygen plasma treatment, the endurance and retention properties of the memory device can be improved by 50% and 25%, respectively. The reason the reliability improved was that Si dangling bonds were repaired to form $SiO_2$ during oxygen plasma treatment. In addition, the process is compatible with the current flash memory fabrication technology.

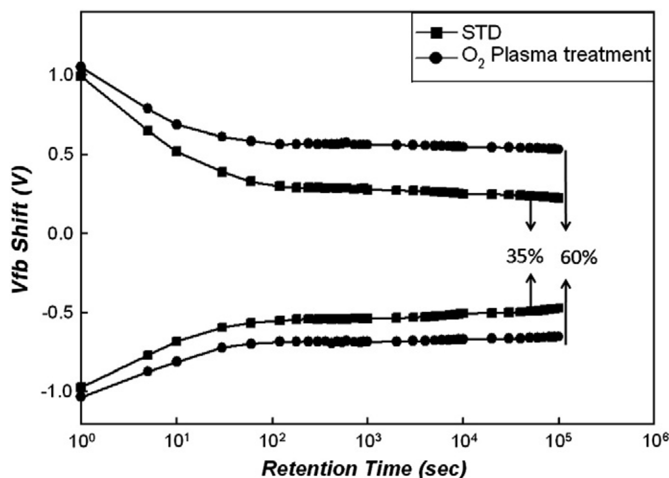


**Fig. 7.** Retention of the tungsten nanocrystal NVMs.

## Acknowledgements

This work was performed at the National Science Council Core Facilities Laboratory for Nano-Science and Nano-Technology in Kaohsiung-Pingtung area and supported by the National Science Council of the Republic of China under Contract Nos. NSC-98-3114-M-110-001 and NSC 97-2112-M-110-009-MY3.

## References

[1] H.E. Maes, J. Witter, G. Groeseneken, Proc. 17 European Solid State Devices Res. Conf. Bologna, 1987, p. 157, 1998.
[2] S. Tiwari, F. Rana, K. Chan, H. Hanafi, C. Wei, D. Buchanan, IEEE Int. Electron. Devices Meet. Tech. Dig. (1995) 521.
[3] H.G. Yang, Y. Shi, S.L. Gu, B. Shen, P. Han, R. Zhang, Y.D. Zhang, Microelectron. J. 34 (2003) 71.
[4] P.H. Yeh, L.J. Chena, P.T. Liu, D.Y. Wang, T.C. Changd, Electrochim. Acta 52 (2007) 2920.
[5] C.H. Chen, T.C. Chang, I.H. Liao, P.B. Xi, Joe Hsieh, Jason Chen, Tensor Huang, S.M. Sze, U.S. Chen, J.R. Chen, Appl. Phys. Lett. 92 (2008) 013114.
[6] C.H. Chen, T.C. Chang, I.H. Liao, P.B. Xi, C.T. Tsai, P.Y. Yang, Joe Hsieh, Jason Chen, U. S. Chen, J.R. Chen, Appl. Phys. Lett. 91 (2007) 232104.
[7] P. Chakraborty, S.S. Mahato, T.K. Maiti1, S. Saha, C.K. Maiti, Proceedings of the International Conference on Nano and Microelectronics (ICONAME 2008), vol. 3–5, Pondicherry Engineering College, Puducherry, India, 2008, p. 239.
[8] Wei-Ren Chen, Ting-Chang Chang, Jui-Lung Yeh, S.M. Sze, Chun-Yen Chang, J. Appl. Phys. 104 (2008) 094303.
[9] Wei-Ren Chen, Ting-Chang Chang, Jui-Lung Yeh, S.M. Sze, Chun-Yen Chang, Appl. Phys. Lett. 92 (2008) 152114.
[10] Chao-Cheng Lin, Ting-Chang Chang, Chun-Hao Tu, Wei-Ren Chen, Chih-Wei Hu, Simon M. Sze, Tseung-Yuen Tseng, Sheng-Chi Chen, Jian-Yang Lin, Appl. Phys. Lett. 93 (2008) 222101.
[11] S.P. Murarka, Silicides for VLSI Applications, Academic Press, INC., London, 1983 3–4.
[12] Houssa 9M., M. Tuominen, M. Naili, V. Afanas'ev, A. Stesmans, S. Haukka, M.M. Heyns, J. Appl. Phys. 87 (2000) 8615.
[13] W.R. Chen, T.C. Chang, P.T. Liu, P.S. Lin, C.H. Tu, C.Y. Chang, Appl. Phys. Lett. 90 (2007) 112108.
[14] Y. Matsushita, S. Samata, M. Miyashita, H. Kubota, IEDM 94 (1994) 321.
[15] Yeong-Shyang Lee, Hsiao-Yi Lin, Tan-Fu Lei, Tiao-Yuan Hung, T.-C. Chang, Chun-Yen Chang, J. J. Appl. Phys. 37 (1998) 3900.
[16] M. Katoh, T. Takbda, J. J. Appl. Phys. 43 (2004) 7297.
[17] H. QIU, Y.F. LU, J. J. Appl. Phys. 39 (2000) 5889.
[18] L.G. Piper, W.T. Rawlins, J. Chem. Phys. 90 (1986) 320.
[19] R. Wolf, K. Wandel, Surf. Coat. Technol. 74–75 (1995) 522.
[20] O. Kubaschewski, B.E. Hopkins, Oxidation of Metals and Alloys, 1953 Butterworths, London.
[21] A. Ikeda, T. Sadou, H. Nagashima, K. Kouno, N. Yoshikawa, K. Tshukamoto, Y. Kurok, Thin Solid Films (1999) 172.